

University of Dundee

Pseudo-ductile Failure of Adhesively Joined GFRP Beam-Column Connections

Ascione, Francesco; Lamberti, Marco; Razaqpur, A. Ghani; Spadea, Saverio; Malagic, Mirfet

Published in:
Composite Structures

DOI:
[10.1016/j.compstruct.2018.05.104](https://doi.org/10.1016/j.compstruct.2018.05.104)

Publication date:
2018

Licence:
CC BY-NC-ND

Document Version
Peer reviewed version

[Link to publication in Discovery Research Portal](#)

Citation for published version (APA):

Ascione, F., Lamberti, M., Razaqpur, A. G., Spadea, S., & Malagic, M. (2018). Pseudo-ductile Failure of Adhesively Joined GFRP Beam-Column Connections: An Experimental and Numerical Investigation. *Composite Structures*, 200, 864-873. <https://doi.org/10.1016/j.compstruct.2018.05.104>

General rights

Copyright and moral rights for the publications made accessible in Discovery Research Portal are retained by the authors and/or other copyright owners and it is a condition of accessing publications that users recognise and abide by the legal requirements associated with these rights.

- Users may download and print one copy of any publication from Discovery Research Portal for the purpose of private study or research.
- You may not further distribute the material or use it for any profit-making activity or commercial gain.
- You may freely distribute the URL identifying the publication in the public portal.

Take down policy

If you believe that this document breaches copyright please contact us providing details, and we will remove access to the work immediately and investigate your claim.

Accepted Manuscript

Pseudo-ductile Failure of Adhesively Joined GFRP Beam-Column Connections: An Experimental and Numerical Investigation

F. Ascione, M. Lamberti, A.G. Razaqpur, S. Spadea, M. Malagic

PII: S0263-8223(18)30107-7

DOI: <https://doi.org/10.1016/j.compstruct.2018.05.104>

Reference: COST 9743

To appear in: *Composite Structures*

Received Date: 9 January 2018

Revised Date: 26 April 2018

Accepted Date: 18 May 2018



Please cite this article as: Ascione, F., Lamberti, M., Razaqpur, A.G., Spadea, S., Malagic, M., Pseudo-ductile Failure of Adhesively Joined GFRP Beam-Column Connections: An Experimental and Numerical Investigation, *Composite Structures* (2018), doi: <https://doi.org/10.1016/j.compstruct.2018.05.104>

This is a PDF file of an unedited manuscript that has been accepted for publication. As a service to our customers we are providing this early version of the manuscript. The manuscript will undergo copyediting, typesetting, and review of the resulting proof before it is published in its final form. Please note that during the production process errors may be discovered which could affect the content, and all legal disclaimers that apply to the journal pertain.

Pseudo-ductile Failure of Adhesively Joined GFRP Beam-Column Connections: An Experimental and Numerical Investigation

Ascione F⁽¹⁾, Lamberti M⁽²⁾, Razaqpur AG^(3,*), Spadea S⁽⁴⁾, Malagic M⁽⁵⁾

(1) Dept. of Civil Engineering, University of Salerno, Italy, email: *fascione@unisa.it*

(2) Dept. of Civil Engineering, University of Salerno, Italy, email: *malamberti@unisa.it*

(3) College of Environmental Science and Engineering, Nankai University, Tianjin, China, email: *GRazaqpur@nankai.edu.cn*

(4) School of Science and Engineering, University of Dundee, United Kingdom, email: *s.spadea@dundee.uk*

(5) Fiberline Composites A/S. Barmstedt Allé 5. DK-5500 Middelfart, email: *mma@fiberline.com*

**Corresponding author*

Abstract

Glass Fiber Reinforced Polymer (GFRP) I-beam-column adhesively bonded connections are tested under combined bending and shear. The special feature of the novel connection is the wrapping of the seat angles at the connection by a carbon fiber reinforced polymer (CFRP) fabric wrap.

The wrap is primarily intended to alter the connection failure mode from brittle to pseudo-ductile, thus providing adequate warning of impending failure. Four moment resisting connection configurations are tested, including the reference configuration without the wrap. It is observed that the connection failure is initiated by the fracture of the adhesive, but the provision of the wrap, together with a steel seat angle, alters the failure mode from brittle to pseudo-ductile. The post-peak load deformation is achieved without a large drop in the resistance of the connection. On other hand, the connection with the wrapping and a GFRP seat angle can also change the failure mode to pseudo-ductile, but it could not be done without a large reduction in the connection resistance after the peak load.

Keywords: Pseudo-ductility, Failure, Adhesive Connections, GFRP, Carbon Wrap, Mechanical Testing

Introduction

Pultruded Glass Fibre Reinforced Polymer (GFRP) profiles are used in construction thanks to their well-known properties such as lightness, high resistance to aggressive chemicals, superior fatigue life and electromagnetic neutrality [1-3]. Typical structures constructed from GFRP include footbridges and industrial buildings while more recent applications involve low-rise residential buildings and temporary structures built for emergency situations. Research has demonstrated possible solutions for mitigating some of the structural problems many emanating from the high deformability of GFRP [4,5] and its negligible plastic capacity [6,7]. Nevertheless, GFRP profiles are not customarily used for building frames due to lack of confidence in the structural performance of frame beam-to column connection.

As currently available GFRP pultruded profiles mimic similar steel sections, most of the research carried out so far on GFRP beam-column connections is focused on adapting the design and construction methods for similar connections in steel structures. For example, Bank and Mosallam [8,9] investigated the performance of GFRP beam-column connections using bolts, web clips and pultruded seat angles between the flanges of the column and the beam. Subsequently, in order to avoid the failure mode initiated by the separation of the column web from the facing flange,

additional angles were used between the web and the flange of the column to strengthen the connection region. In a third junction configuration, GFRP stiffeners were used in both the beam and the column in the neighbourhood of the connection to avoid local compression failure of the flanges.

Based on their test results, they concluded that the design of beam-column connections in pultruded FRP members require careful consideration and it is not appropriate to build FRP frame connections in the same way as steel frame connections. Consequently, Mosallam et al. in [10,11] developed a built-up GFRP connecting element, termed “universal connector”, which was designed to be bolted to the beam flanges and the adjacent column flange. They demonstrated the good performance of this connector as they reported a nearly threefold increase in the connection strength compared to the standard seat angle connector.

Subsequently, Bank et al. [12] modified the universal connector by wrapping a GFRP sheet around the angle, rendering it akin to a hollow wedge. The modified wedge-shaped element yielded the best combination of strength, stiffness and failure mode among all the connection types up to that time.

In 1998, Smith et al. [13] investigated the connection of FRP hollow structural members and indicated that due to the reduced sensitivity of closed sections to distortions, hollow beam connections perform much better than similar I-beam connections. The beam-column connections tested by Smith et al. were similar to the ones tested by Bank and Mosallam, except steel bolts were used instead of GFRP bolts, and in one case, the GFRP seat angles were replaced by steel angles.

In 1999, Smith et al. [14] presented the findings of an experimental investigation demonstrating the performance of their proposed new T-shape monolithic connector, termed “cuff”. The element was used to connect GFRP box beams and columns and led to substantial increases in joint stiffness (90%) and strength (330%), compared to the earlier typical seat angle connections used to join GFRP I-beams and columns. The concept behind the cuff connection is that the beam and column can be inserted inside the cuff, ideally requiring only epoxy adhesive to keep them in place, albeit Smith et al. used both steel bolts and epoxy adhesive to attach the members to the cuff.

In the same years, Mottram et al. [15,16] conducted an experimental investigation on an inner beam-column connection, involving two cantilever beams connected to a central column, with the aim of studying the behavior of web-cleated and flange-cleated beam-to-column connections. Both the beams and the column were made of GFRP I-profiles and the connection was made using GFRP seat angles and steel bolts. As a follow up to the latter two studies, Qureshi et al. in [17-19] investigated the effect of the number and location of required steel or GFRP bolts on the connection performance. They concluded that in the connections involving steel cleats failure is initiated by the general failure of the column while in those involving GFRP cleats, it is induced by local delamination in the column flange above the cleats.

Recently, Zhang et al. [20] and Wu et al. [21] investigated a new bonded sleeve connection suitable for connecting hollow GFRP profiles to steel members. The GFRP beam was fastened to the steel column by steel bolts. They concluded that the end plate thickness is the most influential parameter insofar as the initial stiffness and the bending capacity of the bonded sleeve are concerned.

Martins et al. [22] developed an innovative beam-to-column bolted connection system for GFRP tubes, comprising purpose-built steel connection elements to be inserted into the GFRP hollow sections. Four different bolt configurations were tested, including the number and distance of the bolts from the connected beam end. They included (i) one bolt per web, (ii) two bolts per flange and short end distance, (iii) four bolts per flange, (iv) two bolts per flange and a longer end distance. They concluded that the maximum rotational stiffness was provided by the configuration (iii) and

the maximum failure load by configuration (iv).

All the abovementioned investigations focused on bolted connections using steel bolts alone or steel bolts combined with epoxy adhesive. In an earlier investigation, [23], the authors experimentally investigated for the first time the behavior of full-scale bolt-free GFRP epoxy bonded beam-to-column moment resisting connections under static load. Both the beam and the column had I-profile with dimensions of 200x100x10 mm. Four beam-to column connection prototypes were tested. In all cases, the beam flanges and web were epoxy bonded to the column compression flange by 50x50x6 mm seat angles, with 100 mm length in the case of angles connecting the beam and column flanges and 170 mm when connection beam web to column flange. The test parameters considered were the location of the connection with respect to the free end of the column and the column strengthening method (Figure 1).

The connections are designated as BTCJ_*fc*, BTCJ_*fcr*, BTCJ_*fcm* and BTCJ_*fcmr*, where BTCJ stands for Beam-to-Column Junction, *fc* for flange connection, the letters *m* and *r* for middle and reinforced, respectively.

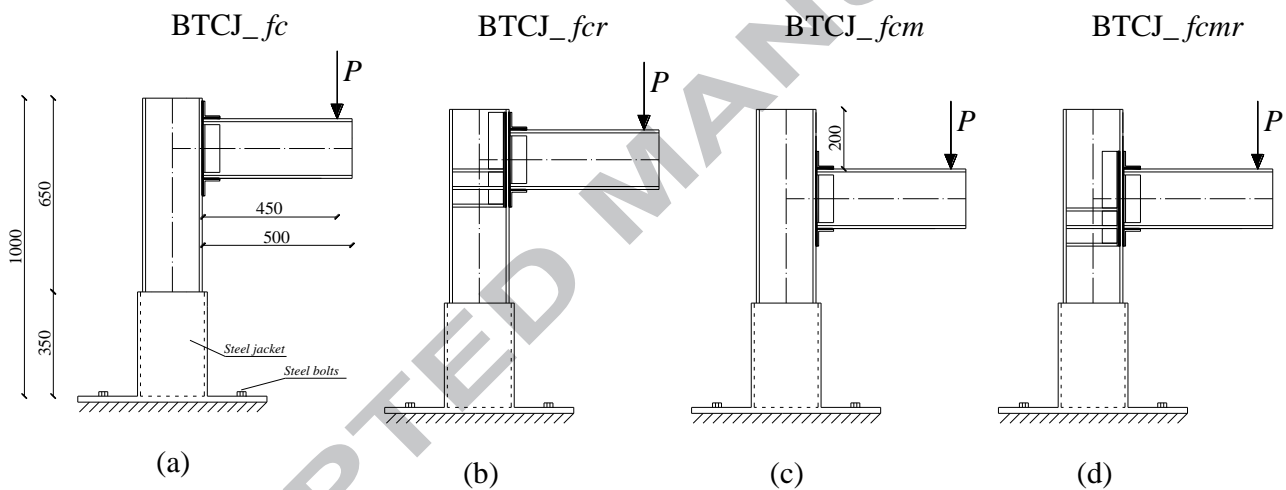


Figure 1. Details of the beam-column connections tested: a) BTCj_*fc*, b) BTCj_*fcr*, c) BTCj_*fcm* and d) BTCj_*fcmr*.

As shown in Figure 1b and 1d, to avoid premature failure of the column, in two cases the column was strengthened in the connection region with adhesively bonded pultruded GFRP strips (45x10 mm, 170 long) and angles (50x50x6 mm, 350 mm long). The results showed that the tested connections possessed strength comparable to the corresponding bolted connections, irrespective of whether steel or GFRP bolts are used. The connections involving seat angles and column stiffeners achieved nearly the same percentage of the GFRP profile ultimate moment capacity as achieved by the best performing bolted connections previously tested by others.

Based on the results of the latter tests, and considering connection strength as the governing design criterion, the prohibition in the current guidelines against the use of adhesive beam-column connections in GFRP frame structures does not seem justified. However, a key disadvantage of the adhesive connection seems to be its brittle failure mode initiated by the failure of the adhesive layer, which may render it less desirable in building structures. Its other disadvantages include, limited deformation capacity (undesirable for earthquake resistance) and its loss of strength and stiffness at elevated temperatures, characteristics that are particularly relevant to ambient-cured adhesives.

To overcome the first drawback of adhesive connections, in the current investigation the authors' previously proposed connection [23] is modified with the aim of changing its failure mode from

brittle to pseudo-ductile. The modification involves wrapping the connection at specific locations with a carbon fiber fabric using epoxy resin and the wet lay-up technique. Laboratory tests are carried out to demonstrate the efficacy of the proposed modification. Simultaneously, finite element analyses are conducted to predict crack initiation and propagation within the adhesive layers in the connection and to investigate whether the observed pseudo-ductile response can be numerically predicted. The experimental and corresponding numerical results are compared and discussed.

Experimental Program

Material characterization tests

Prior to testing the modified connection, the basic mechanical properties of all GFRP elements used in the experiments were determined by means of small-scale coupon tests. Specifically, the apparent interlaminar shear strength τ_M was determined according to the EN ISO 14130:1997 [24] procedures. The in-plane compressive properties, namely, the elastic modulus, E_c , and the compressive strength, σ_{cM} , in both the longitudinal, or pultrusion, and the transverse direction were determined according to the EN ISO 14126:1999 [25]. Similarly, the GFRP tensile modulus, E_t , and strength, σ_{tM} , in both the longitudinal and transverse directions were determined according to EN ISO 527-4:1999 [26]. To obtain the relevant GFRP properties in the transverse direction, the producer of the GFRP profiles used in this experimental program, supplied for testing purpose 500mmx500mmx10mm GFRP plates, with nominally identical composition and manufacturing technique as the tested GFRP profiles. The results of the foregoing tests are reported in Table 1. As expected, the GFRP exhibited a transversally isotropic behaviour with higher strength and stiffness in the pultrusion direction. The lower values in the transverse direction may be explained by the relatively low fiber volume in this direction, with the fibers contributed by the GFRP mat used to facilitate fabrication of the profiles.

Beam-to-column connection test specimens

As stated earlier, in the current investigation, the best performing connection among the ones previously reported by the authors [23] (Figure 2a) was modified by using a carbon fiber fabric impregnated with an epoxy resin. Specimens thus wrapped will be denoted as CFRP wrapped. The tensile elastic modulus and strength of the unidirectional CFRP composite wrap, as reported by the manufacturer, are 220 GPa and 3200 MPa, respectively. With reference to Figures 2b to 2d, three different strengthening methods were investigated.

The modified connections are designated as BTCj_fcrw, BTCj_fcrww, and BTCjs_fcrww, where:

- BTCj stands for beam-to-column junction;
- fcr for reinforced flange connection (the reinforcement consists of angles bonded to web/flange connection of the column)
- w and ww for carbon fabric wrapping around the column and around both the column and the beam, respectively.
- the letter s stands for steel angles.

Each wrapping comprised four layers of carbon fabric: the first strengthening method (BTCj_fcrw) involved wrapping of the column in the tensile zone of the connection, i.e. above the top flange of the beam (Figure 2b); the second method (BTCj_fcrww) involved wrapping of the column above the beam top flange, beam cross-section in the vicinity of the connection as well as the upper seat angle, forming a closed section (Figure 2c); the third method (BTCjs_fcrw) was similar to the

second one, except the upper and bottom GFRP seat angles (50x50x6) were replaced by 50x100x7 mm steel angles.

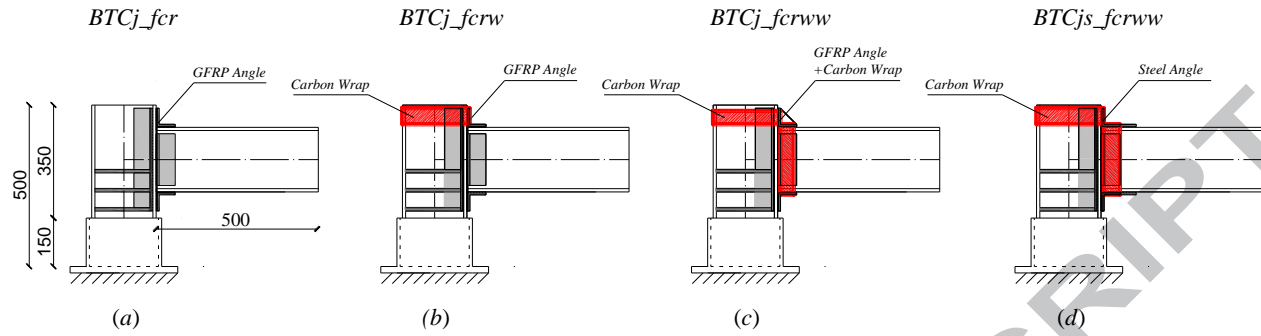


Figure 2. Details of the beam-column connections tested: a) BTCj_fcr, b) BTCj_fcrw, c) BTCj_fcrww and d) BTCjs_fcrww.

The key parameters of the test were the wrap location and the type of seat angles. In total, eight full scale specimens were identically tested (two per each type). As illustrated in Figures 2, unlike the 1000 mm long beam and columns used to make the test specimens in [23], in the current tests the length of the column and the beam were reduced to 500 mm to avoid potential failure outside the connection region.

Table 1. Mechanical properties of GFRP material tested.

Test	Method	Property	Average \pm Std. dev.	Unit
Interlaminar shear	EN ISO 14130:1997	τ_M	34 ± 1.2	MPa
Compression	EN ISO 14126:1999	$E_{c,11}$	19084 ± 330.58	MPa
		$\sigma_{cM,11}$	228 ± 20.08	MPa
		$E_{c,22}$	8500 ± 121.95	MPa
		$\sigma_{cM,22}$	65 ± 4.55	MPa
		$E_{t,11}$	36467 ± 1114.57	MPa
Tension	EN ISO 527-4:1999	$\sigma_{tM,11}$	370 ± 1.31	MPa
		$E_{t,22}$	10569 ± 1679.47	MPa
		$\sigma_{tM,22}$	61 ± 20.31	MPa
		$\nu_{12M,11}$	0.23 ± 0.015	[-]
		$\nu_{12M,22}$	0.09 ± 0.019	[-]

11: pultrusion direction; 22: transverse direction.

For the sake of simplicity, the geometry of all GFRP elements used to realize the beam-to-column specimens of Figure 2 are summarized in Table 2.

Table 2. Geometry of all GFRP elements used.

Shape Profile	Cross Section Dimensions	Length
[-]	[mm x mm x mm]	[mm]
I	200 x 100 x 10	500.0
L	50 x 50 x 6	100.0
L	50 x 50 x 6	170.0
L	50 x 50 x 6	350.0

Plate (strip)	45 x 10	170.0
---------------	---------	-------

The SikaDur 30 epoxy used for bonding the wrapping was the same as the one used by the writers in their previous investigation [23]. It was cured for seven days at temperature ranging between 10 and 15 °C. This temperature range is within the allowable curing temperature specified by the epoxy producer, but lower than the 22-28 °C used by the writers in their previous investigation. After full curing, the epoxy's tensile and shear strengths are specified as 24 and 14MPa, respectively [29].

Test set-up and procedure

As shown in Figure 3a, five displacement transducers (DT1 to DT5) were used to measure each specimen displacements at selected locations for evaluating the connection deformation and stiffness. Transducer DT5 was placed directly below the applied loading point for the purpose of measuring the vertical displacement of the beam near its free end while DT1 to DT4 were used to measure

horizontal displacements at the connection, which will be used to compute the joint rotation and stiffness.

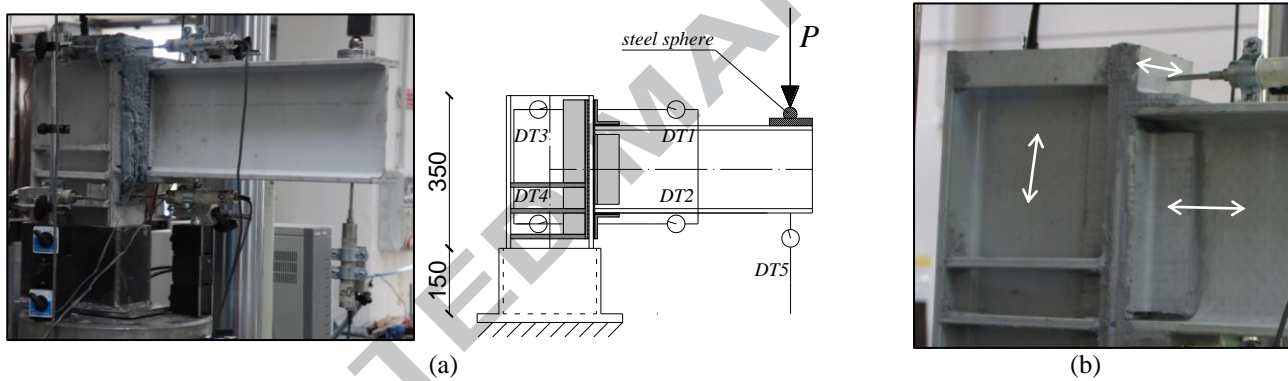


Figure 3. a) Instrumentation set-up, b) pultrusion direction indicated by double headed arrows.

In addition, two strain gauges were installed on the faces of the CFRP wrap parallel to the beam axis to measure wrap strain along its fibers and to estimate the force resisted by the wrap.

The column was inserted into a 150 mm high stiff steel jacket welded to a thick steel plate that was clamped into the testing machine (see Figure 3a). The column fitted snugly inside the jacket and the small gap (1 mm) between them was filled by steel shims. Hence, for all practical purposes, the column can be considered fixed at the bottom with its unsupported length being 350 mm. With reference to Figure 3a, the beam and column assembly was load by a point load applied near the free end of the beam at 450 mm from the column flange connected to the beam. The load was transferred through a 20 mm diameter sphere seated in a circular cavity inside a 50 mm diameter plate which rested on the beam top flange (Figure 4).

The beam was loaded monotonically in displacement control at a rate of 1.0 mm /minute by means of a steel arm clamped to the servo-controlled universal testing machine. All data were automatically and continuously captured.

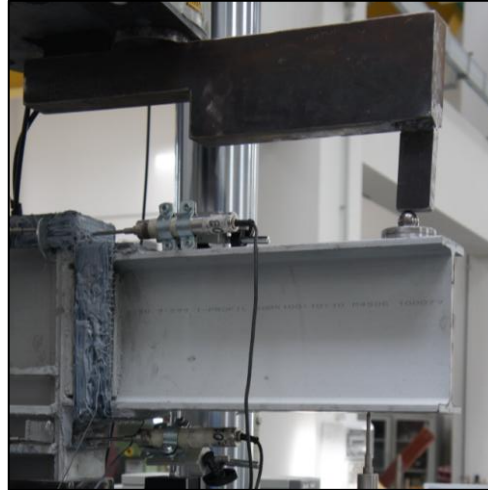


Figure 4. Load application setup.

Results and discussion

In the following, the load versus displacement curves, the moment versus rotation curves as well as the failure mechanism of the tested specimens are presented and discussed.

Load-vertical displacement curves

The beam load-displacement curves for the three CFRP wrapped and the reference (unwrapped) specimen are plotted in Figures 5. Note, the plotted curves show the average response of the two replicate specimens for each connection as the difference between them was found to be relatively small.

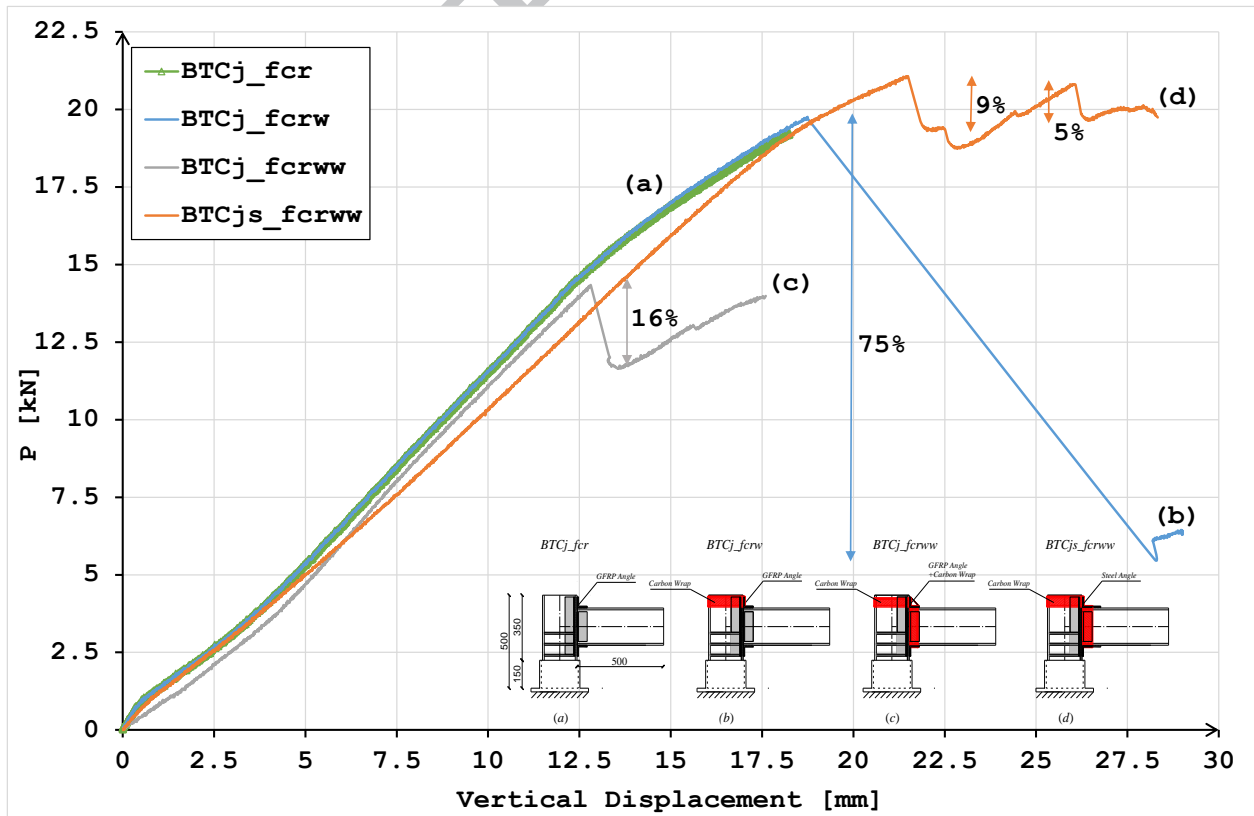


Figure 5. Load vs displacement curves: for specimens BTCj_fcr, BTCj_fcrw, BTCj_fcrww and BTCjs_fcrww.

The curves indicate that the introduction of the wrap did not lead to a consistent or large increase in

the connection strength, but it did change its mode of failure. In particular, connection (d) in Figure 5 exhibited not only the highest strength, but also a “pseudo-ductile” behavior, unlike the brittle failure observed in all the specimens previously tested in [23] and in the current reference specimen. More specifically, connection (b) in Figure 5 showed a similar behaviour to the one shown by the reference connection (a) up to the peak load (about 20 kN). This means that the CFRP wrapping was not able to augment the adhesive strength and increase the connection capacity. On the other hand, the recorded strains, to be shown later, revealed that the CFRP wrapping contributed to the connection strength after the peak load, with the peak load coinciding with fracture incidence in the adhesive layer, Figure 6b. After reaching its peak value, the load dropped drastically to 25% of its peak value, but due to the presence of the CFRP wrapping started to increase again. As can be observed in Figure 6d, at the end of the test (stopped before the failure) the upper seat angle was completely distorted and the vertical leg of the angle was damaged due to compression. This observation underlines the limited contribution to the strength by the such an angle whose fibers were orientated along the width of the column (or of the beam) as depicted in Figure 3b.

The latter observation suggests that the upper seat angle should be strengthened by turning it into a closed section as illustrated in Figure 2(c). Specimen (c) in Figure 5 had a lower peak load but the load dropped less precipitously (only 16%) after its peak value. Whereas the smaller drop may be due to “closed” seat angle, the lower maximum load may be due to the observed slip that occurred between the seat angle and the upper flange of the beam (see Figure 7).

The final connection type tested, i.e. connection (d) in Figure 5, involved steel rather than GFRP angles. As can be seen in the latter figure, it exhibits a pre-peak load behavior similar to the other three types of connections. However, after reaching the peak load of about 21 kN, the load dropped only 9% and subsequently increased and reached the original peak load, followed by another drop of 5%; thereafter, remaining almost constant up to failure.

The smaller drop in load values and the larger deformability of the connection in the latter case may be ascribed to the presence of the steel angles. As mentioned in the case of connection (b), the carbon wrap was fully engaged only after the failure of the adhesive layer joining the beam and the column as manifested by the carbon wrap strain in Figures 8a and its rupture in Figure 8b. No distortion was observed in the steel angles, but the failure was characterized, Figure 8c, by the complete separation of the two structural elements as well as the detachment of the GFRP mat and pull out of fibers from the column flange.

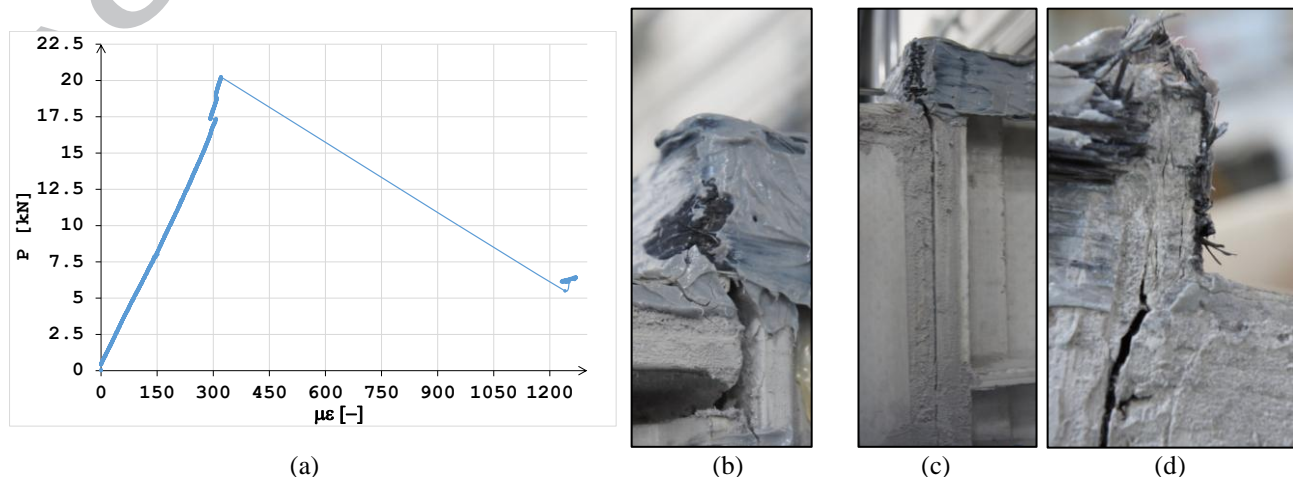
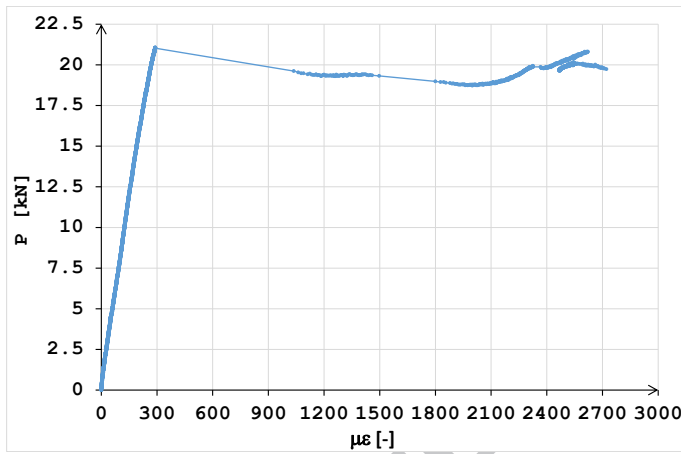


Figure 6. BTCj_fcrw joint: (a) load vs strain curve; (b) initial crack in the adhesive; (c) crack evolution in the adhesive layer; (d) upper seat angle distortion.



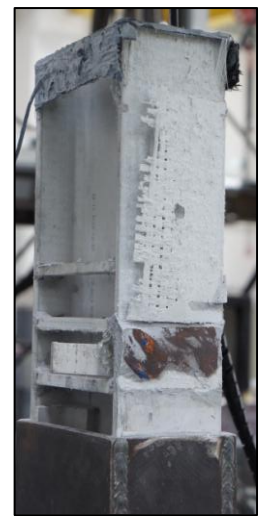
Figure 7. BTCj_fcrww: slip between “closed” seat angle and the upper flange of the beam.



(a)



(b)



(c)

Figure 8. BTCjs_fcrww joint: (a) load vs strain curve; (b) initial crack in the adhesive; (c) failure.

Moment-rotation curves

Two methods are used to analyse the moment-rotation behavior of the tested connections. Figure 9 illustrates the overall rotational stiffness of the beam-column assembly, which is computed by dividing the difference of horizontal displacements measured by transducers DT1 and DT2 by the vertical distance (275 mm) between the two measurement points. The curves exhibit an initial seating of the specimen followed by a clearly linear behaviour. As the load is increased, slight nonlinearity is observed due to the progressive failure of the adhesive joining the two members. For this reason, the slope of the middle linear segment of the moment-rotation curves is considered for comparing the stiffness of tested connections. The average rotational stiffness is computed to be 250 kN·m/rad.

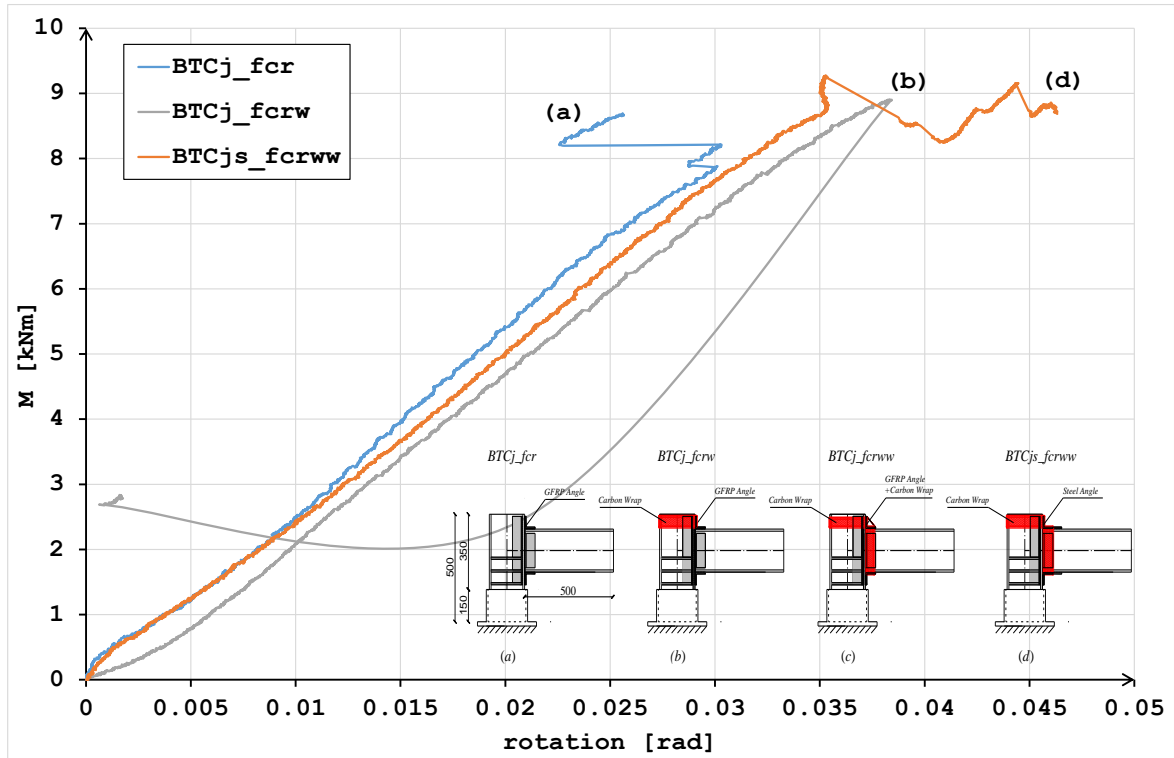


Figure 9. Moment vs rotation curves for specimens BTCj_fcr, BTCj_fcrw, BTCj_fcrww and BTCjs_fcrww.

The moment versus adhesive connections rotation is reported in Figure 10. This is computed by considering the relative horizontal displacement measured by displacement transducers DT 1-3 and DT 2-4 and dividing their sum by the vertical distance (275 mm) between measuring points. It is evident that specimen BTCJs_fcrww is significantly stiffer than BTCJ_fcrw.

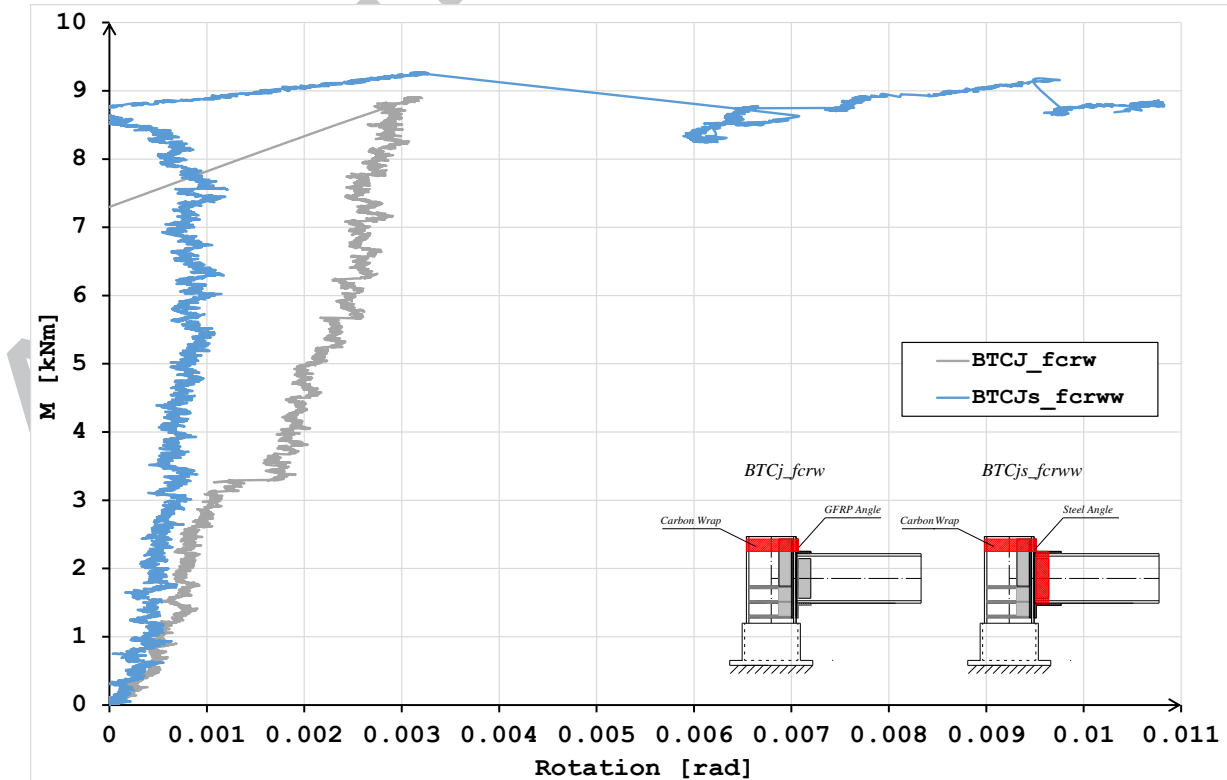


Figure 10. Adhesive connection rotation for specimens BTCj_fcrw and BTCjs_fcrww.

Design standards classify connections rigidity according to their moment-rotation behavior or rotational stiffness. As no standards are available for adhesive connections, they may be classified according to the classification guide provided by Eurocode 3 for steel structures [27]. The code specifies the following categories for elastic analysis: (i) nominally pinned joints, in which no moment is considered to be transmitted through the joint; (ii) rigid joints, in which the connections can be assumed to be fully fixed (no rotations); and (iii) semi-rigid joints, in which the stiffness of the connections needs to be taken into account in the analysis. The classification can be quantitatively carried out using the criteria in Table 3. The symbols E , I_x and L stand for the tensile modulus, the second moment of area and the free bending length of the beam, respectively. For the current specimens their values are, 36467 MPa, $23.6 \times 10^6 \text{ mm}^4$ and 900 mm, respectively. Using the latter values, the boundaries of the rigidity classifications are 478 kN·m/rad and 23906 kN·m/rad. The adhesive joints stiffnesses, K_{aj} , relative to the basic joint (Figure 2b) and strengthened joint with steel angles (Figure 2d), were equal to 3000 kN·m/rad and 8000 kN·m/rad, respectively. Therefore, the proposed bonded connections may be classified as semi-rigid. Since the design of GFRP structures is often governed by serviceability limit state, the possibility to build semi-rigid connections may be beneficial for the structural design. The connection that exhibited the best performance among the ones tested by the authors (BTCjs_fcrww) had ten times higher stiffness than the upper limit of “nominally pinned” and about three times lower than the lower limit of “rigid” connection.

Table 3. Equations for the connection classification.

Rigidity	Classification Criterion	Rigid $K_{aj} \geq 25 E \cdot I_x / L$	Semi-Rigid $25 E \cdot I_x / L > K_{aj} \geq 0.5 E \cdot I_x / L$	Nominally pinned $K_{aj} < 0.5 E \cdot I_x / L$
----------	--------------------------	---	--	--

“Pseudo-ductile” behavior

The pseudo-ductility index was evaluated for all the tested adhesive connections using the method used by Martins et al. [22], originally presented by Iorissen and Fragiacomio [28] for nailed connections involving a brittle material such as wood. The displacement ductility index, μ , is defined as the ratio of the displacement occurring from yielding till failure to the total displacement at failure,

$$\mu = \frac{d_u - d_y}{d_u} \quad (1)$$

where d_y and d_u are the yielding and failure displacements. Ductility is the characteristic of a material undergoing plastic deformations, but since non-plastic or non-ductile materials do not exhibit plasticity, they are characterized by a pseudo-ductility displacement index which is calculated using Eqn (1), but the yield displacement is replaced by the displacement corresponding to the first peak load while the failure displacement is assumed equal to the displacement corresponding to the last peak load of the load-displacement curve (just before the CFRP rupture). It should be pointed out that pseudo-ductility is not a measure of a material plastic behavior, rather it is an indicator of the post-peak load residual strength and concomitant deformation after significant damage in the material, component or connection. The values of μ for the current tested connections are reported in Table 4.

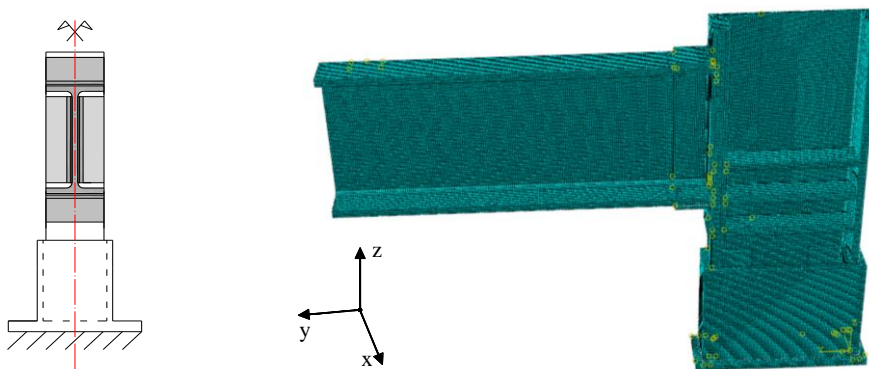
Table 4. Pseudo-ductility index for all connections tested.

Connection	d_u [mm]	d_y [mm]	μ [-]
BTCj_fcr	18.0	13.0	0.00
BTCj_fcrw	29.1	13.0	0.55
BTCj_fcrww	17.6	12.54	0.29
BTCjs_fcrww	28.3	17.0	0.40

Since the control connection (BTCj_fcr) experienced a sudden failure, its failure displacement was taken as the maximum displacement measured. Based on the results reported in Table 4, the beneficial effect of the CFRP wrap is manifested by the over 200% increase in the magnitude of the displacement corresponding to the first peak load the case of BTCj_fcrw connection (GFRP angles) and more than 166% in the case of BTCj_fcrww connection (steel angles).

Numerical simulations

In order to better understand the CFRP wrap contribution to the connection strength and stiffness, and the observed distortion of the upper angle, a non-linear finite element simulation involving large deformations was performed using the Abaqus commercial package. All the GFRP joint components were modeled by eight-node cube elements (C3D8) with 2.5 mm side length. Only the thickness of angles were modeled by eight-node parallelepiped elements (3 x 2.5 mm). The meshes details are summarized in Table 5. The used mesh was found to be the most suitable based on a sensitivity analysis conducted to monitor the vertical displacement of the free end of the beam. The contact between adhesive surfaces was modelled by cohesive laws, both in Mode I, while the contact between GFRP and the steel jacket (bottom of the column) was modeled using the hard contact formulation with no friction. The column was then considered fully fixed at the bottom. The constitutive model adopted for the GFRP elements was transversally isotropic with the relevant mechanical properties as reported in Table 1. Assuming a curing temperature of 15 °C, in compliance with the producer specifications, the adhesive layer tensile and shear strengths were set equal to 24 and 14 MPa, respectively [29]. Due to the presence of a symmetry axis, some simplifications were made in the model (see Figure 11). The analyses were carried out using displacement control, mimicking the experimental procedure used to test connection BTCj_fcr and BTCj_fcrw. Figure 12 shows the normal stresses σ_y (along y axis) and the shear stresses τ_{xz} (in plane xz) distributions in the reference (Figure 12a) and the strengthened connection (Figure 12b) adhesive layer at a load level equal to 50% of each connection failure load.

**Figure 11.** Adhesive connection finite element model.

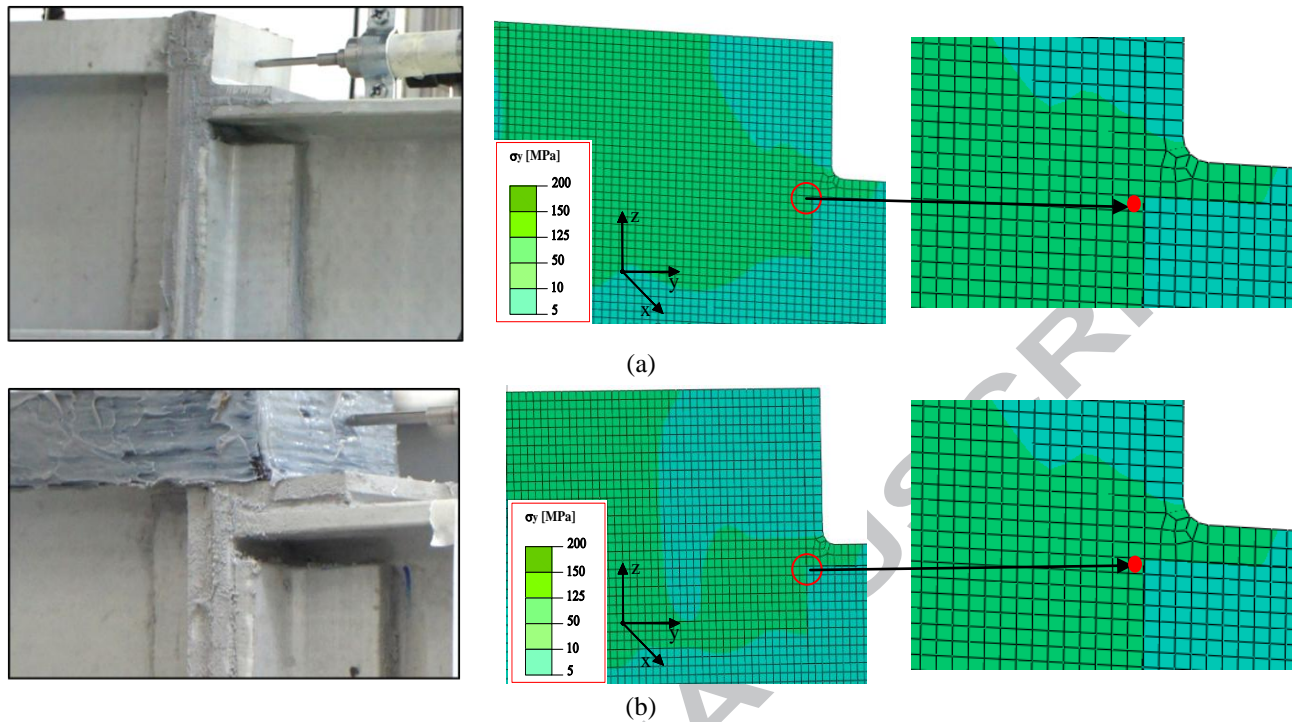


Figure 12. σ_y distribution: (a) BTCj_fcr connection; (b) BTCj_fcrw connection (Load level equal to 50% of the failure load).

Table 5. GFRP element meshes.

Shape Profile [-]	Cross Section Dimensions [mm x mm x mm]	Length [mm]	Elements along the height [mm]	Elements along the width [mm]	Elements along the thickness [mm]	Elements along the length [mm]
I	200 x 100 x 10	500.0	80	40	4	200
L	50 x 50 x 6	100.0	-	20	3	20
L	50 x 50 x 6	170.0	-	20	3	68
L	50 x 50 x 6	350.0	-	20	3	140
Plate (strip)	45 x 10	170.0	-	18	4	68

The carbon fabric was not directly modeled but it was taken into account by assuming a higher adhesive normal strength in the y-direction. This additional strength was evaluated by the load-strain profile depicted in Figure 8a for the connection with steel angles, wherein the highest strain was measured in the carbon wrap compared to the other test specimens. The limit stress value was then quantified by multiplying the observed maximum strain by the Young's modulus of the CFRP wrap. To account for the reduction in strength of the CFRP wrap at its bent corners, the above limit stress was multiplied by a corner efficiency factor of 0.4 as suggested by others [30,31].

The stress distributions of Figure 12 show for the two cases analyzed a concentration of stresses at the bottom corner of the GFRP angle, corroborating the experimentally observed initial cracking starting at this location. In order to simulate the initiation of the fracture and its propagation, the damage initiation criterion of Maximum Nominal Stress (MAXS) was used. The stress components considered are shown in Eq. 2 and when any component equals or exceeds its defined limit or threshold, failure is assumed to have occurred.

$$\max \left\{ \frac{\sigma_y}{\sigma_{0y}}, \frac{\tau_{xz}}{\tau_{0xz}}, \frac{\tau_{yz}}{\tau_{0yz}} \right\} = 1 \quad (2)$$

The symbols σ_{0y} , τ_{0xz} and τ_{0yz} represent the nominal stresses limit (failure criterion) values when the material is subjected to pure normal or shear stress in the specified directions while σ_y , τ_{xz} and τ_{yz} are the actual stress values in the same directions. When the damage initiation criterion is violated, the material response changes in accordance with the chosen bilinear damage evolution law in Mode I, as depicted in Figure 13. This type of constitutive law for adhesive joints is the most accepted and commonly used in the literature [32-35], especially for joints involving FRP [36-38]. The fracture energy was evaluated according to literature (assuming tensile strength of 24 MPa) and the displacement at failure equal to 0.25mm (based on previous test results [37]). The σ_y vs time and τ_{xz} vs time curves, corresponding to the bottom corner of the GFRP angle (locations indicated by the red dots in Figure 12a and 12b) are represented in Figures 14.

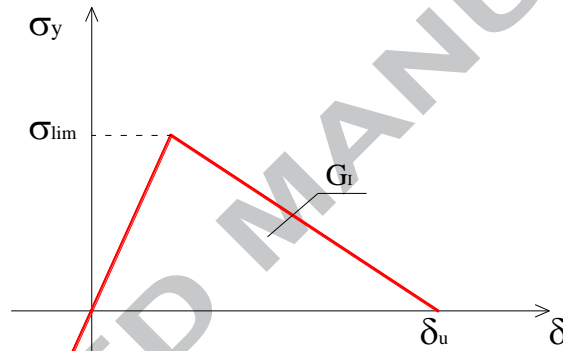


Figure 13. Bilinear constitutive law in Mode I.

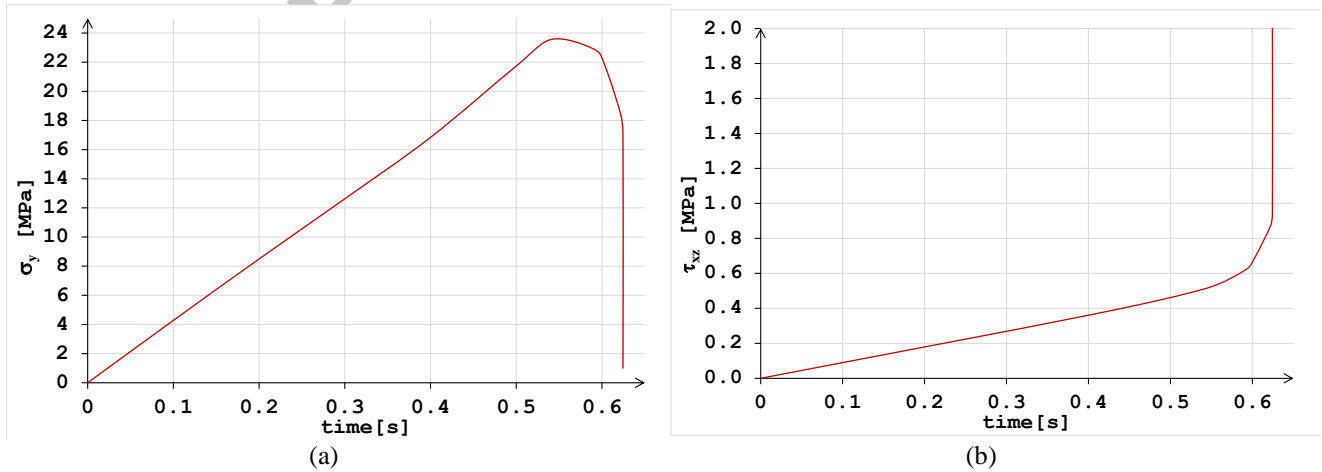


Figure 14. Stress vs time graphs: (a) traction stress σ_y ; (b) shear stress τ_{xz} .

Damage initiation was precipitated by the tensile stress exceeding its 24 MPa limit while the concomitant shear stress of 0.55 MPa was 25 times lower than its limit value of 14 MPa. These results indicate that the present tested connections were subjected to high bending rather than shear stresses.

Finally, the computed crack profile and the corresponding experimental profile at the connection are

shown in Figure 15 and it can be noticed that the two profiles agree well.

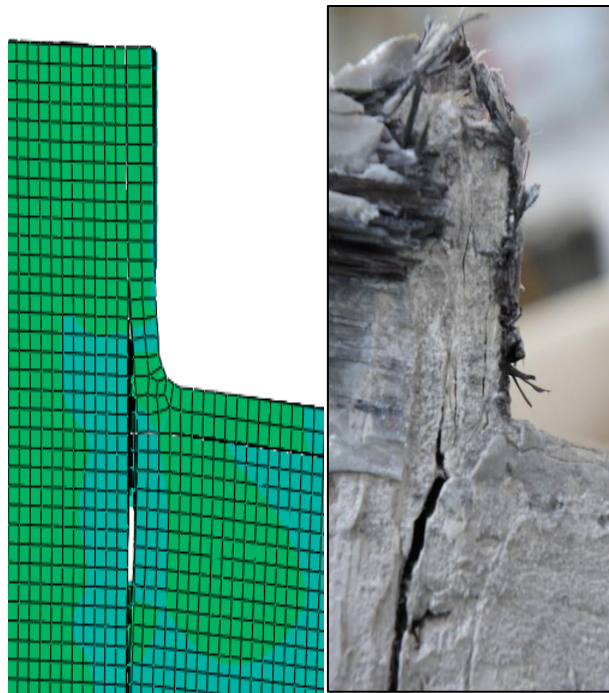


Figure 15. Crack evolution and GFRP seat angle deformations.

Conclusions

In order to avoid sudden and brittle failure of GFRP beam-column connections involving adhesively bonded GFRP clip and seat angles, a CFRP fabric wrap was used to strengthen the connection. The strengthened connection was tested under combined bending and shear and the results support the following conclusions:

- 1) When CFRP strengthening is used, the deformation of the GFRP angles seems to be the factor governing the connection strength.
- 2) The use of the CFRP wrap alters the connection failure mode from a sudden and brittle failure to a more desirable pseudo-ductile mode, without increases the connection strength. The latter mode is characterized by a small reduction of the initial peak load resisted by the connection, followed by a subsequent increase in deformation and load, reaching the initial peak load. This characteristic provides adequate warning of impending connection failure.
- 3) The use of steel versus GFRP seat angles, increases the rotational stiffness of the connection.

Acknowledgments

The authors thank Eng. Massimo Galluzzo, master student at the Department of Civil Engineering at the University of Salerno, for his assistance during the preparation and testing of the specimens.

References

- [1] Fiberline handbook. <http://www.fiberline.com>.
- [2] Report EUR 27666 EN. Prospect for new guidance in the design of FRP. JRC Science for Policy Report (<https://ec.europa.eu/jrc/en/publication/eur-scientific-and-technical-research-reports/prospect-new-guidance-design-frp>).
- [3] Minghini F, Bedon C, Ascione F, Calautit JK. Editorial for the “FRP Structures” Special Issue. American Journal of Engineering and Applied Sciences 2016; 9: 439-441.
- [4] Ascione, L., Berardi, V.P., Giordano, A., Spadea, S. Local buckling behavior of FRP thin-walled beams: A mechanical model (2013) Composite Structures, 98, pp. 111-120.
- [5] Ascione, L., Berardi, V.P., Giordano, A., Spadea, S. Buckling failure modes of FRP thin-walled beams (2013) Composites Part B: Engineering, 47, pp. 357-364.
- [6] Boscato, G. Comparative study on dynamic parameters and seismic demand of pultruded FRP members and structures (2017) Composite Structures, 174, pp. 399-419.
- [7] Noh, J., Ghadimi, B., Russo, S., Rosano, M. Assessment of FRP pultruded elements under static and dynamic loads (2017) Composite Structures, in Press.
- [8] Bank LC, Mosallam AS, Gonsoir HE. Beam-to-column connections for pultruded FRP structures. Suprenant B editor. Serviceability and durability of construction materials, Proceedings of the First Materials Engineering Congress, Denver, CO, 13-15 August, ASCE, 1990:804-813.
- [9] Bank LC, Mosallam AS, McCoy GT. Design and performance of connections for pultruded frame structures. Journal of Reinforced Plastics and Composites 1996;15:1052-1067.
- [10] Mosallam AS. Stiffness and strength characteristics of PFRP UC/beam-to-column connections. Composite material technology, PD-vol.53, Proceedings, ASME Energy-Sources Technology Conference and Expo, TX, 31 January-4 February, 1993: 275-283.
- [11] Mosallam AS, Abdelhamid MK, Conway JH. Performance of pultruded FRP connections under static and dynamic loads. Journal of Reinforced Plastics and Composites 1994;13:386-407.
- [12] Bank LC, Yin J, Moore L. Experimental and numerical evaluation of beam-to-column connections for pultruded structures. Journal of Reinforced Plastics and Composites 1996;15:1052-1067.
- [13] Smith SJ, Parsons ID, Hjelmstad KD. An experimental study of the modeling of connections for pultruded GFRP I-beams and rectangular tubes. Journal of Composites for Construction 1998; 42: 281-290.
- [14] Smith SJ, Parsons ID, Hjelmstad KD. Experimental comparisons of connections for GFRP pultruded frames. Journal of Composites for Construction 1999; 3: 20-26.
- [15] Mottram JT, Zheng Y. Further tests on beam-to-column connections for pultruded frames: web-cleated. Journal of Composite for Construction 1999; 3: 3-11.
- [16] Mottram JT, Zheng Y. Further tests of beam-to-column connections for pultruded frames: flange-cleated. Journal of Composites for Construction 1999; 3: 108-116.
- [17] Qureshi J, Mottram JT. Behaviour of pultruded beam-to-column joints using steel web cleats. Thin-Walled Structures 2013; 73: 48-56.
- [18] Qureshi J, Mottram JT. Response of Beam-To-Column Web Cleated Joints For FRP Pultruded Members. Journal of Composite Construction 2014; 18.
- [19] Qureshi J, Mottram JT. Moment-rotation response of nominally pinned beam-to-column joints for frames of pultruded fibre reinforced polymer. Construction and Building Materials 2015; 77: 396-403.
- [20] Zhang Z, Wu C, Nie X, Bai Y, Zhu L. Bonded sleeve connections for joining tubular GFRP beam to steel member: Numerical investigation with experimental validation. Compos Struct

	2016; 157: 51–61.
[21]	Wu C, Zhang Z, Yu B. Connections of tubular GFRP wall studs to steel beams for building construction. <i>Composites Part B</i> 2016; 95: 64-75.
[22]	Martins D, Proença, Correia JR, Gonilha J, Arruda M, Silvestre N. Development of a novel beam-to-column connection system for pultruded GFRP tubular profiles. <i>Compos Struct</i> 2017; 171: 263–276.
[23]	Ascione F, Lamberti M, Razaqpur AG, Spadea S. Strength and stiffness of adhesively bonded GFRP beam-column moment resisting connections. <i>Compos Struct</i> 2017; 160: 1248–57.
[24]	International Standard EN ISO 14130. Fibre-reinforced plastic composites— Determination of apparent interlaminar shear strength by short-beam method; 1997.
[25]	International Standard EN ISO 14126. Fibre-reinforced composites— Determination of compressive properties in the in-plane direction; 1999.
[26]	International Standard EN ISO 527-4. Test conditions for isotropic and orthotropic fibre-reinforced plastic composites. Determination of tensile properties; 1999.
[27]	Eurocode 3 EN 1993. Design of Steel Structures – Part I-8: Design of Joints. Technical Committee CEN/TC 250.
[28]	Jorissen A, Fragiaco M. General notes on ductility in timber structures. <i>Eng Struct</i> 2011; 33: 2987-2997.
[29]	SikaDur30 technical data sheet (2017) ita.sika.com.
[30]	Lee C., Ko M., Lee Y. Bend strength of complete closed-type carbon fiber-reinforced polymer stirrups with rectangular section. <i>J Compos Constr</i> , 18, 2014.
[31]	Spadea S., Orr J., Ivanova K., Bend-strength of novel filament wound shear reinforcement, <i>Compos Struct</i> , 176, 244-253, 2017.
[32]	Keller T, Vallée T. Adhesively bonded lap joints from pultruded GFRP profiles. Part I: stress–strain analysis and failure modes. <i>Composites Part B</i> 2005; 36:331-40.
[33]	Keller T, Vallée T. Adhesively bonded lap joints from pultruded GFRP profiles. Part II: joint strength prediction. <i>Composites Part B</i> 2005; 36: 311-50.
[34]	Crocombe AD. Modelling and predicting the effects of test speed on the strength of joints made with FM73 adhesive. <i>Int J Adhes Adhes</i> 1995;15: 21–7.
[35]	Abdel Wahab MM, Ashcroft IA, Crocombe AD, Smith PA. Numerical prediction of fatigue crack propagation lifetime in adhesively bonded structures. <i>Int J Fatigue</i> 2002; 24: 705–9.
[36]	Ascione F. Mechanical behaviour of FRP adhesive joints: A theoretical model. <i>Composites Part B</i> 2009; 40: 116-124.
[37]	Ascione F, Feo L, Lamberti M, Penna R. Experimental and numerical evaluation of the axial stiffness of the web to-flange adhesive connections in composite I-beams. <i>Composite Structures</i> 2017; 176: 702-714.
[38]	Ascione F, Mancusi G, Spadea S, Lamberti M, Lebon F, Maurel-Pantel A. On the flexural behaviour of GFRP beams obtained by bonding simple panels: An experimental investigation. <i>Compos Struct</i> 2015; 131: 55-65.